CHEMISTRY
AN ASIAN JOURNAL
www.chemasianj.org

Title: Tertiary Amines Differentiated from Primary and Secondary Amines by Active Ester-Functionalized Hexabenzoperylene in Field Effect Transistors

Authors: Changqing Li, Yujing Wang, Tiankai Zhang, Bo Zheng, Jianbin Xu, and Qian Miao

To be cited as: *Chem. Asian J.* 10.1002/asia.201801787

Link to VoR: http://dx.doi.org/10.1002/asia.201801787

A Journal of
ACES
Asian Chemical Editorial Society

A sister journal of **Angewandte Chemie** and **Chemistry – A European Journal**

WILEY-VCH

Tertiary Amines Differentiated from Primary and Secondary Amines by Active Ester-Functionalized Hexabenzoperylene in Field Effect Transistors

Changqing Li,[1] Yujing Wang,[1] Tiankai Zhang,[2] Bo Zheng,[1] Jianbin Xu,[2] Qian Miao[1] *

Abstract: Herein, we report two novel derivatives of hexabenzoperylene (HBP) that are functionalized with ester groups. Methyl acetate functionalized HBP (**1**) in single crystals self-assembles into a supramolecular nanosheet, which has a two-dimensional π-stack of HBP sandwiched between two layers of ester groups. With the same self-assembly motif, active ester-functionalized HBP (**2**) in field effect transistors has enabled differentiation of tertiary amines from primary and secondary amines, in agreement with the fact that active ester reacts with primary and secondary amines but not with tertiary amines to form amides.

The capability of detecting amines with high sensitivity and selectivity is of key importance to environmental monitoring, medical diagnosis, food quality control and many other applications because amines are ubiquitous in biology, pharmaceuticals, and industry. A variety of techniques have been developed to detect ammonia and amines. [1] Among these techniques, organic field effect transistors (OFETs) offer unique advantages because OFET-based sensors not only circumvent the need for bulky and expensive equipment by combining the sensory electrical output with easy device fabrication, but also promise soft and biocompatible electronics for wearable and implantable devices. [2, 3, 4] The sensing mechanism of the OFET-based sensors for ammonia and amines [5] includes dedoping effect, dipole-charge interaction [6] and chemical gating effect.[7] As a result, these OFET-based sensors generally are not able to achieve high selectivity for different amines. One strategy to enhance selectivity is to introduce binding sites to the surface of organic semiconductors in OFETs. For example, a layer of cucurbit[7]uril on the top of organic semiconductors enabled selective detection of amphetamine-type stimulants in water. [8] Another strategy to enhance the selectivity of OFET-based sensors is to equip organic semiconductors with reactive groups that can react with the analytes. [9, 10] However, this strategy was not reported for OFET-based sensors of amines to the best of our knowledge. Herein, we demonstrate that attachment of active ester to organic semiconductors enables differentiation of tertiary amines from primary and secondary amines.

The organic semiconductor used in this study is hexabenzoperylene (HBP), which is a double [5]helicene.[11] As reported by us earlier, the self-assembly of functionalized HBPs presents an unusual type of two-dimensional π-stacking,[12] which can accommodate a variety of functional groups without sacrificing π-π interactions in the solid state. As a result, functionalized HBPs provide a general sensing platform, which, in a device integrating an OFET channel and a microfluidic channel, has enabled highly sensitive and selective detection of fluoride ions and streptavidin in water.[13] Herein, we report two novel functionalized HBPs, **1** and **2** (Figure 1a). Methyl acetate functionalized HBP **1** with a short linker was found to exhibit the same two-dimensional π-stacking in the crystals as other functionalized HBPs. This crystal structure led us to hypothesize that *p*-nitrophenyl ester functionalized HBP could self-assemble into a π-stacked nanosheet. To test this hypothesis, thin films of **2** were prepared by dip-coating and studied with different techniques. Containing a *p*-nitrophenyl ester group, **2** was designed to differentiate primary and secondary amines from tertiary amines because *p*-nitrophenyl ester reacts with primary or secondary amines (Figure 1b) but does not react with tertiary amines to give amides. By combing an OFET channel with a microfluidic channel, the thin films of **2** have enabled differentiation of primary and secondary amines from tertiary amines as detailed below.

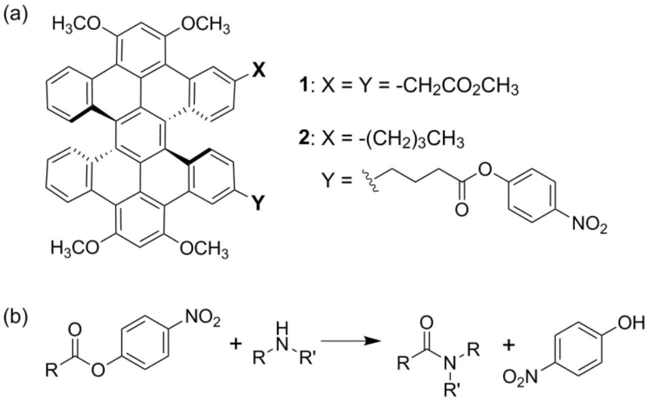

Figure 1. a) Structures of ester functionalized HBPs **1** and **2**; b) reaction of **2** with an amine yielding the corresponding amide.

Ester-functionalized HBPs **1** and **2** were synthesized by modifying the reported synthesis of other functionalized HBPs [13] as shown in Scheme 1. The HBP moiety in **1** and **2** was formed by the Scholl reaction of **5a** and **5b**, respectively, which were synthesized by the Diels-Alder reaction of alkyne **3a** and **3b**, respectively, with cyclopentadienone **4** [14] and the subsequent in-situ decarbonylation. Single crystals of **1** qualified for X-ray crystallography were grown from a solution of **1** in dichloromethane and ethyl acetate by slow evaporation of solvents. As found from the crystal structure, [15] **1** adopts a chiral

---

[a] Dr. C. Li, Y. Wang, Prof. Dr. B. Zheng, Prof. Dr. Q. Miao
Department of Chemistry
The Chinese University of Hong Kong
Shatin, New Territories, Hong Kong, China
E-mail: miaoqian@cuhk.edu.hk
[b] T. Zhang, Prof. Dr. J. Xu
Department of Electronic Engineering
The Chinese University of Hong Kong
Shatin, New Territories, Hong Kong, China
Supporting information for this article is given via a link at the end of the document.

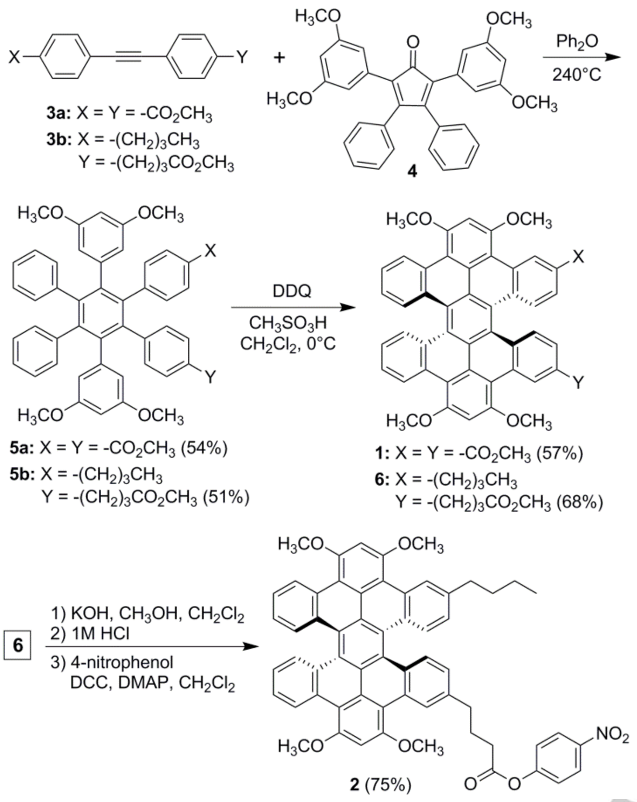

Scheme 1 Synthesis of ester functionalized HBPs **1** and **2**

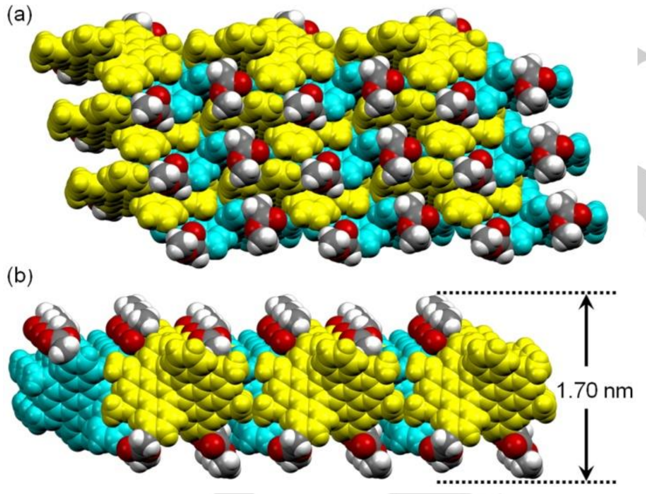

Figure 2. a) A nanosheet of **1** as viewed along the *b* axis of the crystal lattice; b) a nanosheet of **1** as viewed along the *c* axis of the crystal lattice. (The *P*- and *M*-enantiomers, except their ester groups, are shown in yellow and light blue, respectively. Co-crystallized water molecules are removed for clarity.)

twisted conformation having its fjord regions distorted with torsion angles of 42.1° and 40.5°. The crystal of **1** is racemic containing *P*- and *M*-enantiomers, which are shown in yellow and light blue, respectively, in Figure 2a. Each *P*-enantiomer of **1** stacks with four adjacent *M*-enantiomers in a brickwork arrangement, which is essentially the same as those of other functionalized HBPs in crystals. [13] Since the HBP backbone of **1** can be regarded as two roughly planar benzotetracene subunits jointed by the twisted central benzene ring, the face-to-face π-stacking of **1** is along two directions with the same π-to-π distance of 3.6 Å. This packing motif leads to a 1.70 nm-thick supramolecular nanosheet, which has a two-dimensional stack of π-faces sandwiched between two layers of ester groups as shown in Figure 2b. In addition, the crystal of **1** contains co-crystallized water molecules (not shown in Figure 2) between two adjacent nanosheets.

In order to prepare electrical sensors that integrate an OFET channel and a microfluidic channel, thin films of **2** were fabricated by dip coating films of **2** a silicon substrate, which had successive layers of titanium oxide, alumina and 12-methoxylphosphonic acid (MODPA) as a composite dielectric material. Here, MODPA formed a self-assembled monolayer (SAM) on alumina to provide an ordered dielectric surface wettable by common organic solvents.[16] It is worth noting that each step in the dip coating processes in this study, including removal of solvent residues in a vacuum, was conducted at room temperature to avoid thermal isomerization of HBP.[14] The dip-coated films of **2** consisted of well aligned crystalline fibers as found from the reflection polarized light micrograph shown in Figure 3a. In contrast, dip-coating solution of **1** onto the same substrate resulted in isolated thick crystals that were not suitable for fabrication of field effect transistors likely because of the lower solubility of **1**. The fabrication of transistors was completed by vacuum-deposition of gold onto the dip-coated films of **2** through a shadow mask to form top-contact source and drain electrodes. As measured from 16 channels of these devices in air, the film of **2** behaved as a p-type semiconductor with field effect hole mobility in the range of $(3.4 \pm 0.6)\times10^{-2}$ cm^2/Vs. Figure 3b shows transfer I–V curves for a representative transistor of **2** as measured in air. The output curve of the same transistor was displayed in Figure S4 (Supporting Information).

The supramolecular assemblies of **2** in the thin films were studied with UV–vis absorption spectroscopy, X-ray diffraction (XRD), and atomic force microscopy (AFM). The dip-coated film of **2** on glass exhibited a broad absorption band in the visible light region with the longest-wavelength maxima at 570 nm, whereas the solution of **2** in CH_2Cl_2 (1×10^{-5} M) exhibited the longest-wavelength absorption peak at 512 nm as shown in Figure S3 (Supporting Information). The red shifted absorption of **2** in films relative to that in solutions is 58 nm, which is similar to those of functionalized HBPs as reported previously.[12, 13] It can be attributed to electronic delocalization between π-stacked molecules, suggesting strong π–π interactions between the formed π-stacked nanosheets.[17, 18] XRD from the film of **2** on $MOPDA/TiO_x/AlO_x/Si$ substrate exhibited one intense peak at $2\theta = 5.16°$ (*d* spacing of 1.71 nm) accompanied with two higher order peaks at $2\theta = 10.43°$ (*d* spacing of 0.85 nm) and $2\theta = 15.78°$ (*d* spacing of 0.56 nm). These diffractions suggest that the dip-coated film of **2** have a layered nano-structure with each layer of 1.7 nm thick. As found from AFM section analysis (Figure 3c), the fibers of **2** in the dip-coated films were 30.5 to 41.8 nm thick and thus consisted of 18 to 24 of nanosheet layers. Based on the above results, we conclude that molecules of **2** self-assemble into π-stacked nanosheets in the dip-coated films.

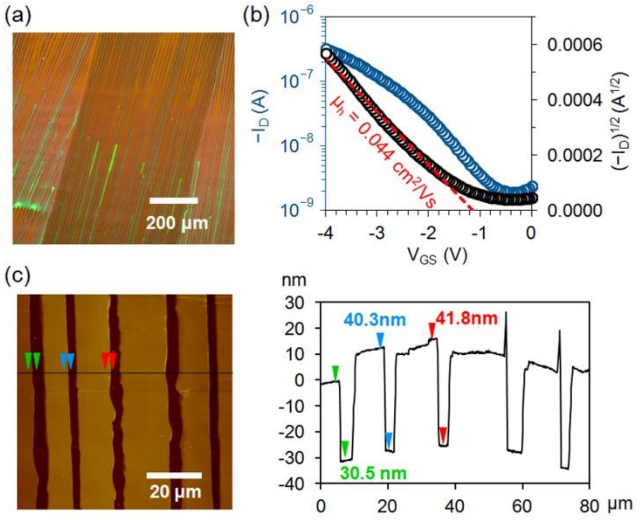

Figure 3. a) Reflection polarized light micrograph for a dip-coated film of **2** on MODPA-modified $TiO_x/AlO_x/Si$; b) transfer curves for a representative OFET of **2** with an active channel of 150 μm long and 1 mm wide as tested in air; c) AFM image and cross-section analysis for a dip-coated film of **2** on MODPA-modified $TiO_x/AlO_x/Si$. (The film of **2** was prepared by immersing the substrate into a solution of **2** in 1:1 (v/v) CH_2Cl_2-ethyl acetate and then pulling it up with a constant speed of 0.15 mm min^{-1}.)

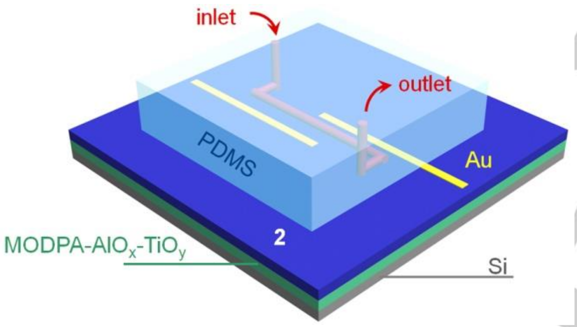

Figure 4. Schematic drawing of the sensor combining a microchannel and a transistor channel (150 μm long and 4 mm wide) of **2**.

Electrical sensors were fabricated by carefully placing a piece of polydimethylsiloxane (PDMS) with preformed microfluidic channels onto the top-contact OFETs of **2** under a microscope so that water in the microfluidic channel contacted the organic semiconductor layer but did not touch the gold electrodes. Figure 4 shows a schematic drawing of this sensor, which is the same as that reported by us earlier except the molecular structure of the organic semiconductor. In this device, the transistor of **2** exhibited good stability when exposed to deionized water for 30 minutes (Figure S5 in the Supporting Information). To test the sensing ability of **2** toward different amines as well as ammonia, a solution of amine or ammonia (0.2 mM) in deionized water was injected into the microchannel using a syringe pump with a speed of 30 µL/min and the flow of the solution was kept for 5 minutes. Before injection of the solution of amine, the microchannel was filled with deionized water for about 30 minutes until the drain current became stable in order to exclude the response of the drain current toward water. The compounds tested in this study included two primary amines (i.*e.*, *n*-hexylamine and phenethylamine), two secondary amines (i.*e.*, diethyl amine and piperidine), and two tertiary amines (triethylamine and pyridine) as well as ammonia. Figure 5a shows the transfer I-V curves of **2** as measured under deionized water and under a solution of *n*-hexylamine for a certain period of time. The drain current (V_{DS} = −4 V and V_{GS} = −4 V) decreased by 19% after the transistor channel was exposed to *n*-hexylamine for 1 minute, and decreased by 30% after 5 minutes. Similarly, after the transistor channel was exposed to diethylamine for 1 minute and 5 minutes, the drain current (V_{DS} = −4 V and V_{GS} = −4 V) decreased by 30% and 49%, respectively, as shown in Figure 5b. In contrast, the drain current did not decrease after exposure of the transistor channel to triethylamine for 1 minute, while exposure to triethylamine for 5 minutes resulted in decrease of the drain current (V_{DS} = −4 V and V_{GS} = −4 V) by 7% as shown in Figure 5c. Figure 5d summarizes the responses of the OFETs of **2** toward different amines as well as ammonia in aqueous solutions, clearly indicating that this sensor can differentiate triethylamine and pyridine from other amines with apparently smaller change of drain current ($\Delta I/I_0$). It was found that replacing the aqueous solution of primary or secondary amines in the microfluidic channel with deionized water did not lead to increase of the drain current. This is in agreement with the irreversible reaction of active ester with amines. In contrast to the device of **2**, the OFET of unfunctionalized HBP **7** [12] was not able to differentiate a tertiary amine from primary and secondary amines as shown in Figure S9 in the Supporting Information. When the OFET channel of **7** was exposed to *n*-hexylamine, diethylamine and triethylamine for 5 minutes, the drain current decreased by 20%. 13% and 16%, respectively, in a control experiment.

The observed decrease of drain current of **2** toward different amines can be attributed to two mechanisms. First, amines that diffuse into the active channel can quench mobile holes by reacting with the cations of **2**.[6] Second, the reaction of the active ester with primary and secondary amines results in the corresponding amide and thus changes the dipole and hydrophilicity of the surface. The first mechanism is applicable to all amines while the second mechanism is only applicable to primary and secondary amines as well as ammonia. In agreement with this, the contact angle of the film of **2** with water decreased more than 10 degrees after exposure to ammonia, hexylamine, phenethylamine, diethylamine and piperidine while only decreased by less than 5 degrees after exposure to triethylamine and pyridine (Figure S6 in the Supporting Information).

In conclusion, methyl acetate functionalized HBP (**1**), similar to other functionalized HBPs, in single crystals self-assembles into a π-stacked supramolecular nanosheet. Active ester functionalized HBP (**2**) in dip-coated films exhibits the same self-assembly motif as revealed by UV–vis absorption spectroscopy, XRD and AFM. The electrical sensor integrating an OFET channel of **2** and a microfluidic channel has enabled differentiation of tertiary amines from primary and secondary amines in water because tertiary amines, unlike primary and secondary amines, do not react with active ester to form amides.

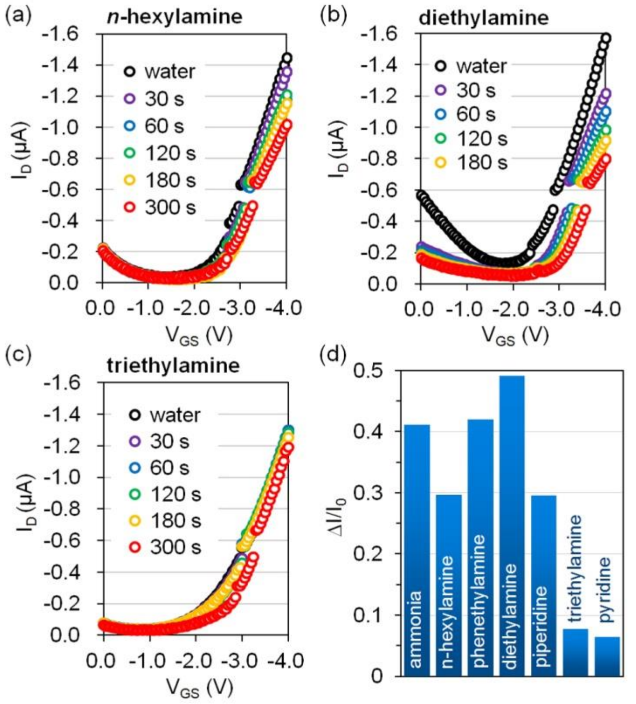

Figure 5 (a–c) Transfer I-V Curves for the OFET of **2** as measured under deionized water and under an aqueous solution (0.2 mM) of *n*-hexylamine (a), diethylamine (b) and triethylamine (c) for a certain period of time; (d) change in the drain current ($\Delta I/I_0$) of **2** in the transfer I-V curve with drain and gate voltage both at −4V as a result of exposure to different amines with the same concentration (0.2mM) in deionized water for 5 minutes.

Acknowledgements

We thank Ms. Hoi Shan Chan (the Chinese University of Hong Kong) for the single crystal crystallography. This work was supported by the Research Grants Council of Hong Kong (project number: GRF14303614) and the Chinese University of Hong Kong (Direct grant 3132677).

Keywords: sensors • organic semiconductors • organic field effect transistors • arenes • self-assembly

[1] a) K. Kivirand, T. Rinken, *Anal. Lett.* **2011**, *44*, 2821–2833; b) M.-S. Steiner, R. J. Meier, A. Duerkop, O. S. Wolfbeis, *Anal. Chem.* **2010**, *82*, 8402–8405; c) Y. Hu, X. Ma, Y. Zhang, Y. Che, J. Zhao, *ACS Sens.***2016**, *1*, 22–25; d) Á. Kovács, L. Simon-Sarkadi, K. Ganzler, *J. Chromatogr. A* **1999**, *836*, 305–313; e) H. S. Mader, O. S. Wolfbeis, *Anal. Chem.* **2010**, *82*, 5002–5004; f) F. Bedia Erim, *Trends Anal. Chem.* **2013**, *52*, 239–247; g) L. V. Jørgensen, H. H. Huss, P. Dalgaard, *J. Agric. Food Chem.* **2001**, *49*, 2376–2381; h) S. F. Liu, A. R. Petty, G. T. Sazama, T. M. Swager, *Angew. Chem., Int. Ed.* **2015**, *54*, 6554–6557; i) C. Lynam, K. Jennings, K. Nolan, P. Kane, M. A. McKervey, D. Diamond, *Anal. Chem.* **2002**, *74*, 59–66.

[2] a) P. Lin, F. Yan, *Adv. Mater.* **2012**, *24*, 34–51; b) Y. Guo, G. Yu, Y. Liu, *Adv. Mater.* **2010**, *22*, 4427–4447; c) G. Tarabella, F. Mahvash Mohammadi, N. Coppedè, F. Barbero, S. Iannotta, C. Santato, F. Cicoira, *Chem. Sci.* **2013**, *4*, 1395; d) L. Torsi, M. Magliulo, K. Manoli, G. Palazzo, *Chem. Soc. Rev.* **2013**, *42*, 8612; e) T. Someya, A. Dodabalapur, J. Huang, K. C. See, H. E. Katz, *Adv. Mater.* **2010**, *22*, 3799–3811; f) X. Wu, S. Mao, J. Chen, J. Huang, *Adv. Mater.* **2018**, *30*, 1705642.

[3] a) T. Someya, Z. Bao, G. G. Malliaras, *Nature* **2016**, *540*, 379–385; b) A. N. Sokolov, B. C.-K. Tee, C. J. Bettinger, J. B.-H. Tok, Z. Bao, *Acc. Chem. Res.* **2012**, *45*, 361–371.

[4] D. Khodagholy, T. Doublet, P. Quilichini, M. Gurfinkel, P. Leleux, A. Ghestem, E. Ismailova, T. Hervé, S. Sanaur, C. Bernard, G. G. Malliaras, *Nat. Commun.* **2013**, *4*, 1575.

[5] a) F. Zhang, C. Di, N. Berdunov, Y. Hu, Y. Hu, X. Gao, Q. Meng, H. Sirringhaus, D. Zhu, *Adv. Mater.* **2013**, *25*, 1401–1407; b) T. Minami, T. Minamiki, K. Fukuda, D. Kumaki, S. Tokito, *Jpn. J. Appl. Phys.* **2015**, *54*, 04DK01; c) N. J. Tremblay, B. J. Jung, P. Breysse, H. E. Katz, *Adv. Funct. Mater.* **2011**, *21*, 4314–4319; d) T. Minamiki, T. Minami, D. Yokoyama, K. Fukuda, D. Kumaki, S. Tokito, *Jpn. J. Appl. Phys.* **2015**, *54*, 04DK02; e) W. Huang, K. Besar, R. LeCover, A. M. Rule, P. N. Breysse, H. E. Katz, *J. Am. Chem. Soc.* **2012**, *134*, 14650–14653; f) Y. Yang, G. Zhang, H. Luo, J. Yao, Z. Liu, D. Zhang, *ACS Appl. Mater. Interfaces* **2016**, *8*, 3635–3643; g) A. N. Sokolov, M. E. Roberts, O. B. Johnson, Y. Cao, Z. Bao, *Adv. Mater.* **2010**, *22*, 2349–2353; h) T. Lau, E. Lorenz, M. Koyuncu, *Jpn. J. Appl. Phys.* **2013**, *52*, 041601; i) H.-W. Zan, W.-W. Tsai, Y. Lo, Y.-M. Wu, Y.-S. Yang, *IEEE Sens. J.* **2012**, *12*, 594–601; j) J. Lu, D. Liu, J. Zhou, Y. Chu, Y. Chen, X. Wu, J. Huang, *Adv. Funct. Mater.* **2017**, *27*, 1700018; k) H.-W. Zan, M.-Z. Dai, T.-Y. Hsu, H.-C. Lin, H.-F. Meng, Y.-S. Yang, *IEEE Electron Device Lett.***2011**, *32*, 1143–1145; l) B. Peng, S. Huang, Z. Zhou, P. K. L. Chan, *Adv. Funct. Mater.* **2017**, *27*, 1700999; m) F. Zhang, G. Qu, E. Mohammadi, J. Mei, Y. Diao, *Adv. Funct. Mater.* **2017**, *27*, 1701117; n) J. Li, B. Lv, D. Yan, S. Yan, M. Wei, M. Yin, *Adv. Funct. Mater.* **2015**, *25*, 7442–7449.

[6] L. Li, P. Gao, M. Baumgarten, K. Müllen, N. Lu, H. Fuchs, L. Chi, *Adv. Mater.* **2013**, *25*, 3419–3425.

[7] H. Chen, S. Dong, M. Bai, N. Cheng, H. Wang, M. Li, H. Du, S. Hu, Y. Yang, T. Yang, F. Zhang, L. Gu, S. Meng, S Hou, X. Guo, *Adv. Mater.* **2015**, *27*, 2113–2120.

[8] Y. Jang, M. Jang, H. Kim, S. J. Lee, E. Jin, J. Y. Koo, I.-C. Hwang, Y. Kim, Y. H. Ko, I. Hwang, J. H. Oh, K. Kim, *Chem* **2017**, *3*, 641–651.

[9] a) J. Huang, J. Miragliotta, A. Becknell, H. E. Katz, *J. Am. Chem. Soc.* **2007**, *129*, 9366–9376; b) K. C. See, A. Becknell, J. Miragliotta, H. E. Katz, *Adv. Mater.* **2007**, *19*, 3322–3327.

[10] L. Torsi, G. M. Farinola, F. Marinelli, M. C. Tanese, O. H. Omar, L. Valli, F. Babudri, F. Palmisano, P. G. Zambonin, F. Naso, *Nat. Mater.* **2008**, *7*, 412–417.

[11] C. Li, Y. Yang, Q. Miao, *Chem. Asian J.* **2018**, *13*, 884–894.

[12] L. Shan, D. Liu, H. Li, X. Xu, B. Shan, J.-B. Xu, Q. Miao, *Adv. Mater.* **2015**, *27*, 3418–3423.

[13] C. Li, H. Wu, T. Zhang, Y. Liang, B. Zheng, J. Xia, J. Xu, Q. Miao, *Chem*, **2018**, 4, 1416–1426.

[14] J. Luo, X. Xu, R. Mao, Q. Miao, *J. Am. Chem. Soc.* **2012**, *134*, 13796–13803.

[15] CCDC 1548512 contains the supplementary crystallographic data for **1**. This data can be obtained free of charge from The Cambridge Crystallographic Data Centre via www.ccdc.cam.ac.uk/data_request/cif.

[16] D. Liu, X. Xu, Y. Su, Z. He, J. Xu, Q. Miao, *Angew. Chem., Int. Ed.* **2013**, *52*, 6222–6227.

[17] Q. Miao, X. Chi, S. Xiao, R. Zeis, M. Lefenfeld, T. Siegrist, M. L. Steigerwald, C. Nuckolls, *J. Am. Chem. Soc.* **2006**, *128*, 1340–1345.

[18] S.-H. Lim, T. G. Bjorklund, F. C. Spano, C. J. Bardeen, *Phys. Rev. Lett.* **2004**, *92*, 107402.

10.1002/asia.201801787

Entry for the Table of Contents

COMMUNICATION

Active ester-functionalized hexabenzoperylene in field effect transistors has enabled differentiation of tertiary amines from primary and secondary amines in water.

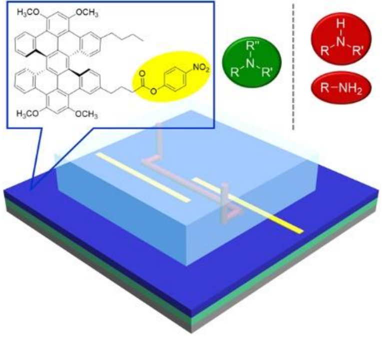

*Changqing Li, Yujing Wang, Tiankai Zhang, Bo Zheng, Jianbin Xu, Qian Miao**

Page No. – Page No.

Tertiary Amines Differentiated from Primary and Secondary Amines by Active Ester-Functionalized Hexabenzoperylene in Field Effect Transistors